Supporting Information

In-situ grown Ni phosphate@$Ni_{12}P_5$ nanorod arrays as unique core-shell architecture: competitive bifunctional electrocatalysts for large current densities urea electrolysis

*Xiujuan Xu, [#] Puyu Du, [#] Tong Guo, Bolin Zhao, Huanlei Wang and Minghua Huang**

[#] *These authors contributed equally to this work*

School of Materials Science and Engineering, Ocean University of China, 238 Songling Road, Qingdao 266100, China

*Corresponding author: huangminghua@ouc.edu.cn

Number of Pages: 12

Number of Figures: 8

Number of Tables: 2

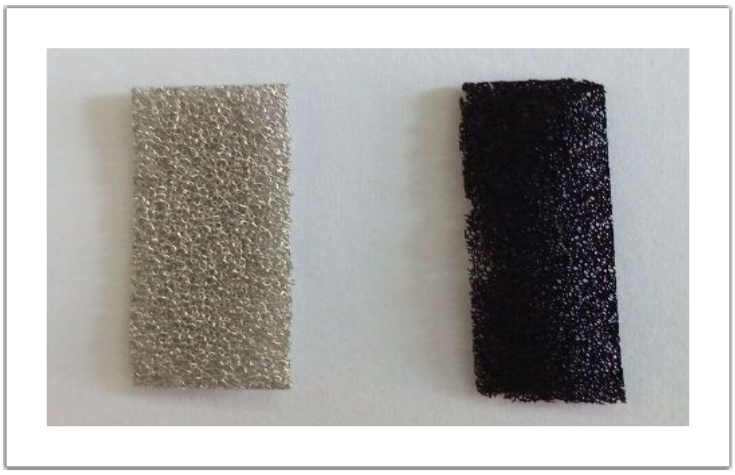

Figure. S1. Optical photographs of the NF (left) and the $Ni_{12}P_5$/Ni-Pi/NF (right).

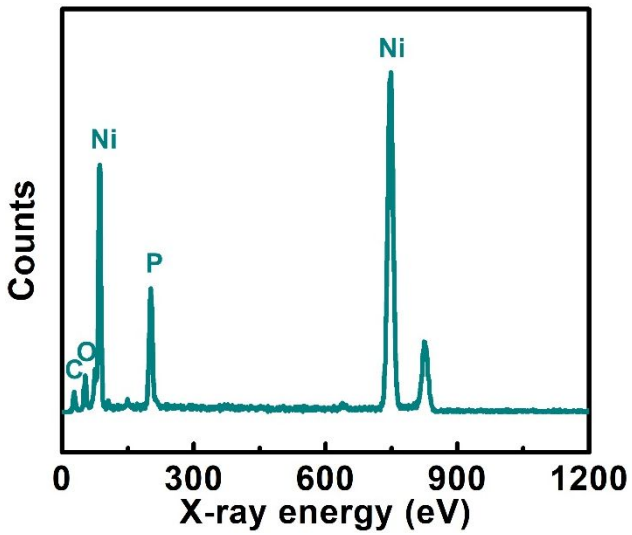

Figure. S2. EDS spectrums for the $Ni_{12}P_5$/Ni-Pi/NF.

Table S1. Comparison of the electrocatalytic UOR activity of the $Ni_{12}P_5$/Ni-Pi/NF with other new electrocatalysts recently reported in alkaline solutions with urea.

Electrocatalyst	j (mA cm^{-2})	Corresponding V vs. RHE	Tafel slope	Electrolyte	Refs
$Ni_{12}P_5$/Ni-Pi/NF	250 500	1.347 1.358	29.0	1M KOH+0.5M urea	This work
$NiCo_2O_4$	136	1.624	-	1M KOH+0.33M urea	[1]
Ni-MOF	10	1.36	23	1M KOH+0.33M urea	[2]
NiO-Fe_2O_3/rGO /PVA	10	1.39	-	1M KOH+0.33M urea	[3]
Ni_2P	10	1.38	49	1M KOH+0.5M urea	[4]
L-MnO_2	10	1.37	89	1M KOH+0.5M urea	[5]
Ni-Zn	60	1.414	-	5M KOH+0.33M urea	[6]
Ni-P	70	1.37	84	1M KOH+0.33M urea	[7]
Ni_2P	10	1.42	78.2	1M KOH+0.33M urea	[8]
CoS_2 NA/Ti	10	1.4	80	1M KOH+0.33M urea	[9]
$Ni(OH)_2$ NS@NW/NF	10	1.407	47	1M KOH+0.33M urea	[10]
NiCoP	50	1.379	117	1M KOH+0.33M urea	[11]
NF@p-Ni	141	1.667	-	1M KOH+0.33M urea	[12]
NiO	800	1.624	-	1M KOH+0.33M urea	[13]
$NiCo_2S_4$ /NF	720	1.228	-	5M KOH+0.33M urea	[14]
Ni^{3+}-rich $Ni(OH)_2$ /C-NH_2	91.72	1.677	-	1M KOH+0.33M urea	[15]
NiO-Ni/NF	10 100	1.347 1.427	55	1M KOH+0.33M urea	[16]
Ni/C-1	100	2.0	-	1M KOH+0.33M urea	[17]
Ni_2P/Fe_2P/NF	10	1.36	79.1	1M KOH+0.5M urea	[18]

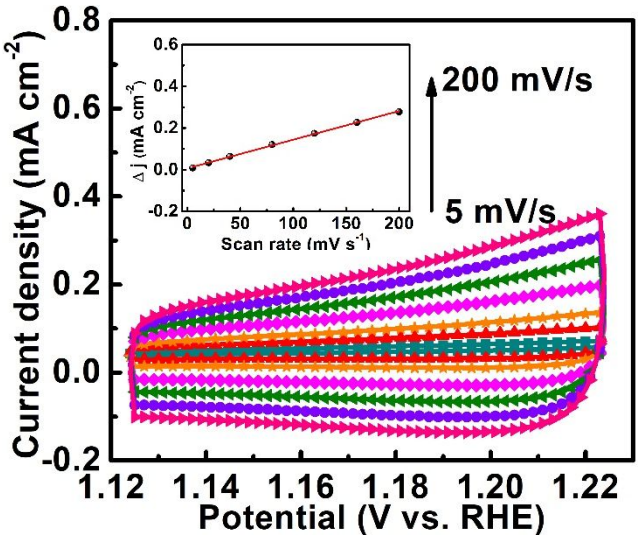

Figure. S3 CVs of bare NF at different scan rates from 5 to 200 mV/s. The inset shows capacitive current density at 1.144 V (vs. RHE) plotted versus scan rate for bare NF.

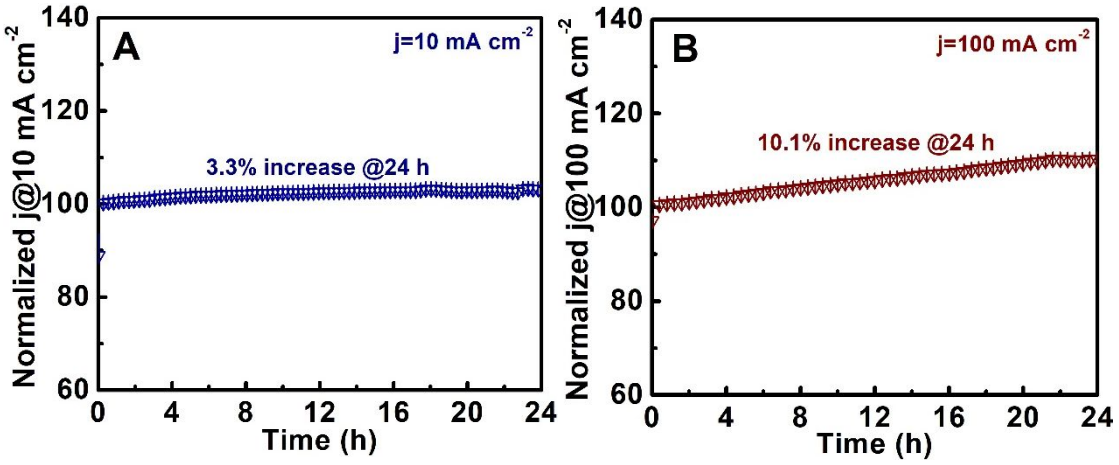

Figure. S4 (A) and (B) The time-dependent potential curve of $Ni_{12}P_5$/Ni-Pi/NF with constant UOR current density of 10 and 100 mA cm^{-2} for 24 h.

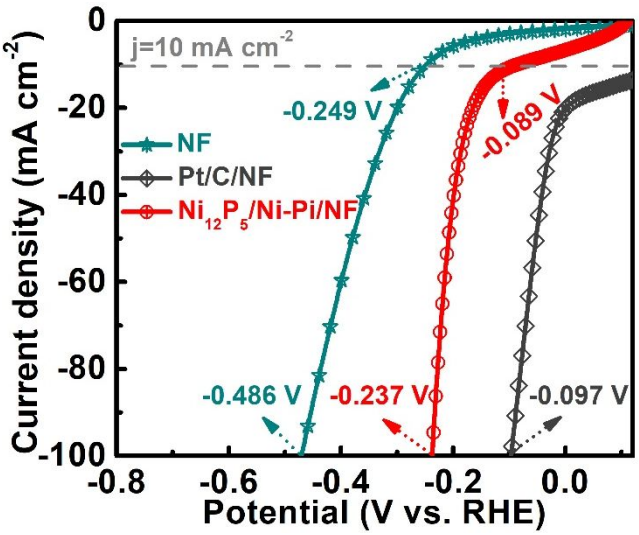

Figure. S5 LSV curves for bare NF, Pt/C/NF and $Ni_{12}P_5$/Ni-Pi/NF in 1.0 M KOH with 0.5 M urea for HER.

Table S2. Comparison of the electrocatalytic overall urea electrolysis performance of the $Ni_{12}P_5$/Ni-Pi/NF//$Ni_{12}P_5$/Ni-Pi/NF with other electrocatalysts couples recently reported in alkaline solutions with urea.

Electrocatalyst Couple	j (mA cm^{-2})	Corresponding V vs. RHE	Electrolyte	Refs
$Ni_{12}P_5$/Ni-Pi/NF// $Ni_{12}P_5$/Ni-Pi/NF	50 500	1.532 1.662	1M KOH+0.5M urea	This work
$NiCo_2S_4$/CC//$NiCo_2S_4$/CC	20	1.55	1M KOH+0.33M urea	[19]
CoS_2 NA/Ti//CoS_2 NA/Ti	10	1.59	1M KOH+0.33M urea	[9]
Ni_3N/CC//Ni_3N/CC	50	1.70	1M KOH+0.33M urea	[20]
MoS_2/Ni_3S_2/Ni/NF// MoS_2/Ni_3S_2/Ni/NF	20	1.45	1M KOH+0.5M urea	[21]
$Ni(OH)_2$ NS@NW/NF// $Ni(OH)_2$ NS@NW/NF	10	1.68	1M KOH+0.5M urea	[10]
S-MnO_2//S-MnO_2	10	1.61	5M KOH+0.33M urea	[5]
MnO_2/$MnCo_2O_4$/Ni// MnO_2/$MnCo_2O_4$/Ni	10	1.55	1M KOH+0.5M urea	[22]
$Fe_{11.1\%}$-Ni_3S_2/NF// $Fe_{11.1\%}$-Ni_3S_2/NF	10	1.46	1M KOH+0.33M urea	[23]
HC-NiMoS/Ti// HC-NiMoS/Ti	10	1.59	1M KOH+0.5M urea	[24]
Ni_2P/CFC//Ni_2P/CFC	10	1.48	1M KOH+0.33M urea	[8]
NiCoP/CC// NiCoP/CC	50	1.62	1M KOH+0.5M urea	[25]
Ni_2P/Fe_2P/NF// Ni_2P/Fe_2P/NF	10	1.47	1M KOH+0.5M urea	[18]

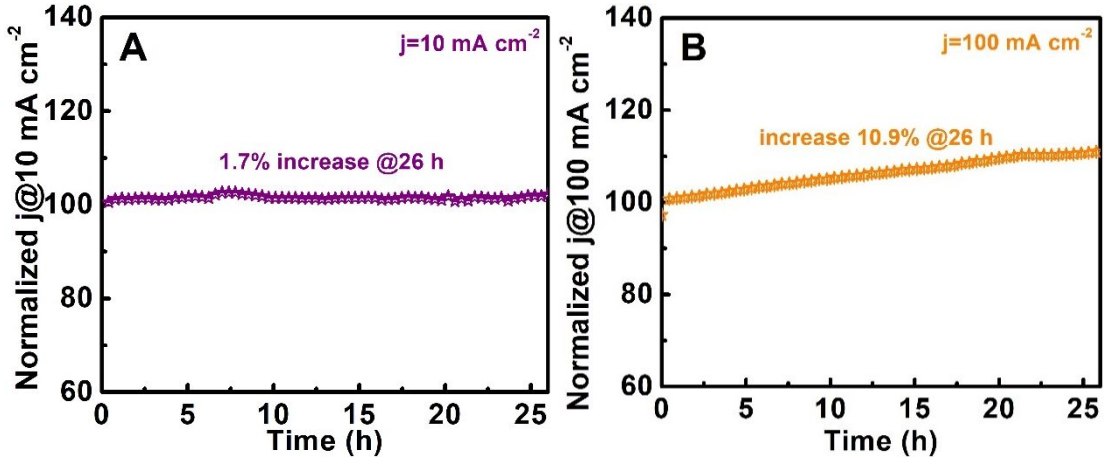

Figure. S6 (A) and (B) The time-dependent potential curve of the $Ni_{12}P_5$/Ni-Pi/NF//$Ni_{12}P_5$/Ni-Pi/NF couple with constant current density of 10 and 100 mA cm^{-2} for 26 h.

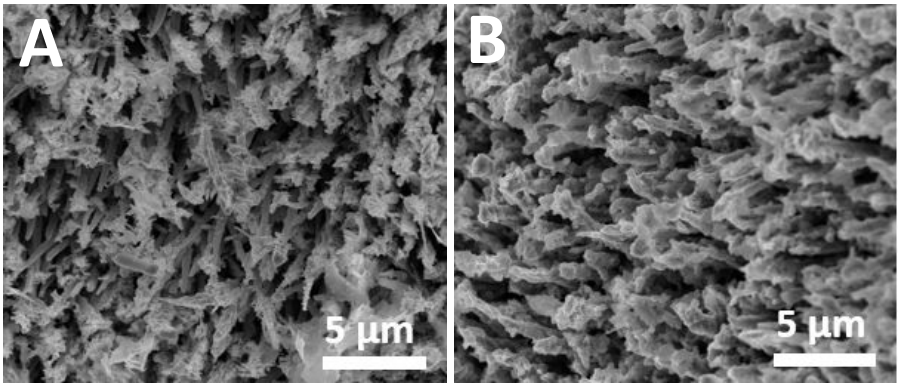

Figure. S7. SEM images for $Ni_{12}P_5$/Ni-Pi/NF after 6 h continuous electrolysis for HER (A) and UOR (B) at 500 mA cm^{-2}.

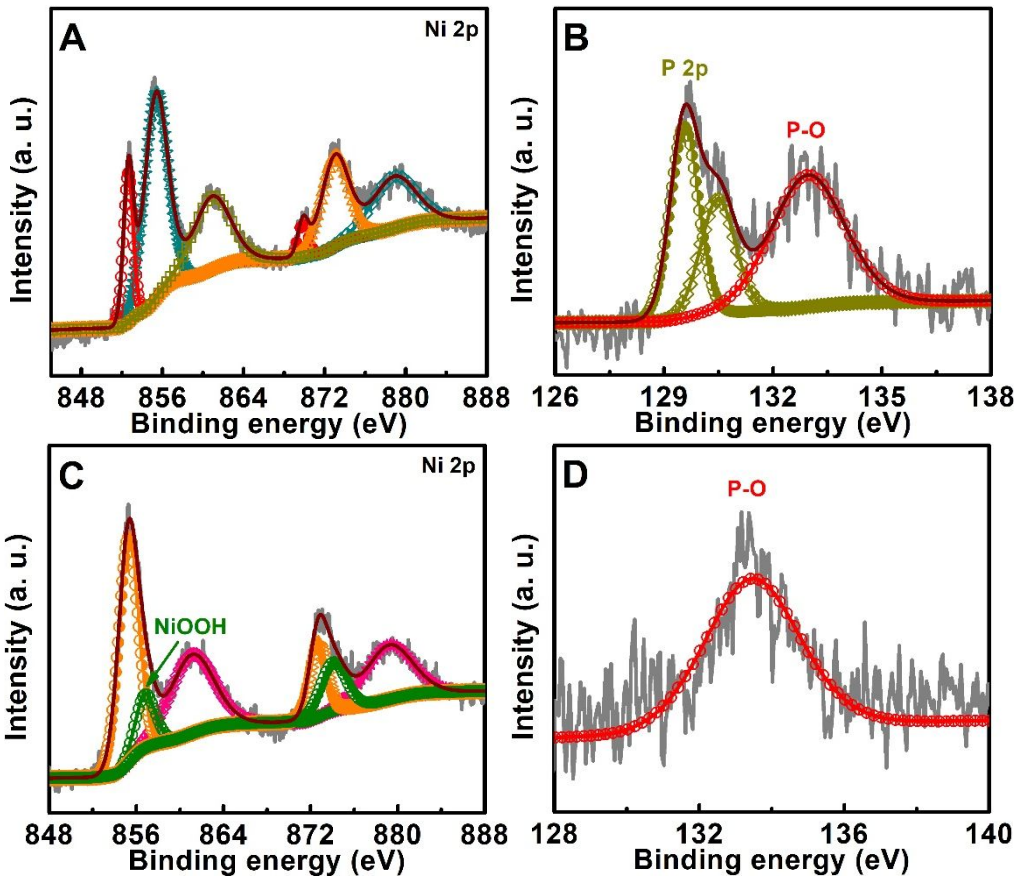

Figure. S8. XPS spectra of (A) Ni 2p and (B) P 2p regions for the $Ni_{12}P_5$/Ni-Pi/NF after 6 h durability test at 500 mA cm^{-2} for HER. XPS spectra of (C) Ni 2p and (D) P 2p regions for the $Ni_{12}P_5$/Ni-Pi/NF after 6 h durability test at 500 mA cm^{-2} for UOR.

References

1. Ding, R.; Qi, L.; Jia, M. J.; Wang, H. Y. Facile synthesis of mesoporous spinel $NiCo_2O_4$ nanostructures as highly efficient electrocatalysts for urea electro-oxidation. *Nanoscale* **2014**, *6*, 1369-1376. DOI 10.1039/c3nr05359h.
2. Zhu, D. D.; Guo, C. X.; Liu, J. L.; Wang, L.; Du, Y.; Qiao, S.-Z. Two-dimensional metal-organic frameworks with high oxidation states for efficient electrocatalytic urea oxidation. *Chem. Commun.* **2017**, *53*, 10906-10909. DOI 10.1039/c7cc06378d.
3. Das, G.; Tesfaye, R. M.; Won, Y. S.; Yoon, H. H. NiO-Fe_2O_3 based graphene aerogel as urea electrooxidation catalyst. *Electrochim. Acta* **2017**, *237*, 171-176. DOI 10.1016/j.electacta.2017.03.197.
4. Liu, D. N.; Liu, T. T.; Zhang, L. X.; Qu, F. L.; Du, G.; Asiri, A. M.; Sun, X. P. High-performance urea electrolysis towards less energy-intensive electrochemical hydrogen production using a bifunctional catalyst electrode. *J. Mater. Chem. A* **2017**, *5*, 3208-3213. DOI 10.1039/c6ta11127k.
5. Chen, S.; Duan, J. J.; Vasileff, A.; Qiao, S. Z. Size fractionation of two-dimensional sub-nanometer thin manganese dioxide crystals towards superior urea electrocatalytic conversion. *Angew. Chem., Int. Ed.* **2016**, *55*, 3804-3808. DOI 10.1002/anie.201600387.
6. Yan, W.; Wang, D.; Botte, G. G. Electrochemical decomposition of urea with Ni-based catalysts. *Appl Catal B:Environm* **2012**, *127*, 221-226. DOI 10.1016/j.apcatb.2012.08.022
7. Ding, R.; Li, X. D.; Shi, W.; Xu, Q. L.; Wang, L.; Jiang, H. X.; Yang, Z.; Liu, E. H. Mesoporous Ni-P nanocatalysts for alkaline urea electrooxidation. *Electrochim. Acta* **2016**, *222*, 455-462. DOI 10.1016/j.electacta.2016.10.198.
8. Zhang, X.; Liu, Y. Y.; Xiong, Q. Z.; Liu, G. Q.; Zhao, C. J.; Wang, G. Z.; Zhang, Y. X.; Zhang, H. M.; Zhao, H. J. Vapour-phase hydrothermal synthesis of Ni_2P nanocrystallines on carbon fiber cloth for high-efficiency H_2 production and simultaneous urea decomposition. *Electrochim. Acta* **2017**, *254*, 44-49. DOI

10.1016/j.electacta.2017.09.097.

9. Wei, S.; Wang, X. X.; Wang, J. M.; Sun, X. P.; Cui, L.; Yang, W. R.; Zheng, Y. W.; Liu, J. Q. CoS_2 nanoneedle array on Ti mesh: a stable and efficient bifunctional electrocatalyst for urea-assisted electrolytic hydrogen production. *Electrochim. Acta* **2017**, *246*, 776-782. DOI 10.1016/j.electacta.2017.06.068.
10. Yue, Z. H.; Yao, S. Y.; Li, Y. Z.; Zhu, W. X.; Zhang, W. T.; Wang, R.; Wang, J.; Huang, L. J.; Zhao, D. Y.; Wang, J. L. Surface engineering of hierarchical $Ni(OH)_2$ nanosheet@nanowire configuration toward superior urea electrolysis. *Electrochim. Acta* **2018**, *268*, 211-217. DOI 10.1016/j.electacta.2018.02.059.
11. Xie, L. S.; Liu, Q.; Luo, Y.; Liu, Z. A.; Xu, Y. T.; Asiri, A. M.; Sun, X. P.; Xie, F. Y. Bimetallic NiCoP Nanosheets Array for High-Performance Urea Electro-Oxidation and Less Energy-Intensive Electrolytic Hydrogen Production. *ChemistrySelect* **2017**, *2*, 10285-10289. DOI 10.1002/slct.201702071.
12. Wu, M.-S.; Sie, Y.-J.; Yang, S.-B. Hollow mesoporous nickel dendrites grown on porous nickel foam for electrochemical oxidation of urea. *Electrochim. Acta* **2019**, *304*, 131-137. DOI 10.1016/j.electacta.2019.02.100.
13. Zhan, S. H.; Zhou, Z. R.; Liu, M. M.; Jiao, Y. L.; Wang, H. T. 3D NiO nanowalls grown on Ni foam for highly efficient electro-oxidation of urea. *Catalysis Today* **2019**, *327*, 398-404. DOI 10.1016/j.cattod.2018.02.049.
14. Sha, L. N.; Ye, K.; Wang, G.; Shao, J. Q.; Zhu, K.; Cheng, K.; Yan, J.; Wang, G. L.; Cao, D. X. Rational design of $NiCo_2S_4$ nanowire arrays on nickle foam as highly efficient and durable electrocatalysts toward urea electrooxidation. *Chem. Eng. J* **2019**, *359*, 1652-1658. DOI 10.1016/j.cej.2018.10.225
15. Wang, D. S.; Liu, S. W.; Gan, Q. P.; Tian, J. N.; Isimjan, T. T.; Yang, X. L. Two-dimensional nickel hydroxide nanosheets with high-content of nickel (III) species towards superior urea electro-oxidation. *J. Electroanal. Chem.* **2018**, *829*, 81-87. DOI 10.1016/j.jelechem.2018.10.007.
16. Yue, Z. H.; Zhu, W. X.; Li, Y. Z.; Wei, Z. Y.; Hu, N.; Suo, Y. R.; Wang, J. L. Surface engineering of a nickel oxide-nickel hybrid nanoarray as a versatile

catalyst for both superior water and urea oxidation. *Inorg. Chem.* **2018**, *57*, 4693-4698. DOI 10.1021/acs.inorgchem.8b00411.

17. Wang, L.; Ren, L. T.; Wang, X. R.; Feng, X.; Zhou, J. W.; Wang, B. Multivariate MOF-templated pomegranate-like Ni/C as efficient bifunctional electrocatalyst for hydrogen evolution and urea oxidation. *ACS Appl. Mater. Interfaces* **2018**, *10*, 4750-4756. DOI 10.1021/acsami.7b18650.
18. Yan, L.; Sun, Y. L.; Hu, E. L.; Ning, J. Q.; Zhong, Y. J.; Zhang, Z. Y.; Hu, Y. Facile in-situ growth of Ni_2P/Fe_2P nanohybrids on Ni foam for highly efficient urea electrolysis. *J. Colloid. Interf. Sci.* **2019**, *541*, 279-286. DOI 10.1016/j.jcis.2019.01.096.
19. Zhu, W. X.; Ren, M. R.; Hu, N.; Zhang, W. T.; Luo, Z. T.; Wang, R.; Wang, J.; Huang, L. J.; Suo, Y. R.; Wang, J. L. Traditional $NiCo_2S_4$ Phase with Porous Nanosheets Array Topology on Carbon Cloth: A Flexible, Versatile and Fabulous Electrocatalyst for Overall Water and Urea Electrolysis. *ACS Sustainable Chem. Eng.* **2018**, *6*, 5011-5020. DOI 10.1021/acssuschemeng.7b04663.
20. Liu, Q.; Xie, L. S.; Qu, F. L.; Liu, Z.; Du, G.; Asiri, A. M.; Sun, X. P. A porous Ni_3N nanosheet array as a high-performance non-noble-metal catalyst for urea-assisted electrochemical hydrogen production. *Inorg. Chem. Front* **2017**, *4*, 1120-1124. DOI 10.1039/c7qi00185a.
21. Li, F.; Chen, J. X.; Zhang, D. F.; Fu, W. F.; Chen, Y.; Wen, Z. H.; Lv, X. J. Heteroporous MoS_2/Ni_3S_2 towards superior electrocatalytic overall urea splitting. *Chem. Commun.* **2018**, *54*, 5181-5184. DOI 10.1039/c8cc01404c.
22. Xiao, C. L.; Li, S.; Zhang, X. Y.; MacFarlane, D. R. $MnO_2/MnCo_2O_4$/Ni heterostructure with quadruple hierarchy: a bifunctional electrode architecture for overall urea oxidation. *J. Mater. Chem. A* **2017**, *5*, 7825-7832. DOI 10.1039/c7ta00980a.
23. Zhu, W. X.; Yue, Z. H.; Zhang, W. T.; Hu, N.; Luo, Z. T.; Ren, M. R.; Xu, Z. J.; Wei, Z. Y.; Suo, Y. R.; Wang, J. L. Wet-chemistry topotactic synthesis of bimetallic iron-nickel sulfide nanoarrays: an advanced and versatile catalyst for

energy efficient overall water and urea electrolysis. *J. Mater. Chem. A* **2018**, *6*, 4346-4353. DOI 10.1039/c7ta10584c.

24. Wang, X. X.; Wang, J. M.; Sun, X. P.; Wei, S.; Cui, L.; Yang, W. R.; Liu, J. Q. Hierarchical coral-like NiMoS nanohybrids as highly efficient bifunctional electrocatalysts for overall urea electrolysis. *Nano Research* **2018**, *11*, 988-996. DOI 10.1007/s12274-017-1711-3.
25. Sha, L. N.; Yin, J. L.; Ye, K.; Wang, G.; Zhu, K.; Cheng, K.; Yan, J.; Wang, G. L.; Cao, D. X. The construction of self-supported thorny leaf-like nickel-cobalt bimetal phosphides as efficient bifunctional electrocatalysts for urea electrolysis. *J. Mater. Chem. A* **2019**, *7*, 9078-9085. DOI 10.1039/c9ta00481e.